Supporting Information for

A Facile Space-Confined Solid-Phase Sulfurization Strategy for Growth of High-Quality Ultrathin Molybdenum Disulfide Single Crystals

Dawei Li,*[,†] Zhiyong Xiao,[‡,§] Sai Mu,[∥] Fei Wang,[⊥] Ying Liu,[†] Jingfeng Song,[‡,§] Xi Huang,[†] Lijia Jiang,[†] Jun Xiao,[†] Lei Liu,[†] Stephen Ducharme,[‡,§] Bai Cui,[§,⊥] Xia Hong,[‡,§] Lan Jiang,[#] Jean-Francois Silvain,[▽] and Yongfeng Lu*[,†]

[†] Department of Electrical and Computer Engineering, University of Nebraska-Lincoln, Lincoln, NE 68588-0511, United States

[‡] Department of Physics and Astronomy, University of Nebraska-Lincoln, Lincoln, NE 68588-0511, United States

[§] Nebraska Center for Materials and Nanoscience, University of Nebraska-Lincoln, NE 68588-0299, United States

[∥] Materials Science and Technology Division, Oak Ridge National Laboratory, Oak Ridge, TN 37831-6124, United States

[⊥] Department of Mechanical & Materials Engineering, University of Nebraska–Lincoln, Lincoln, NE 68588, United States

[#] School of Mechanical Engineering, Beijing Institute of Technology, Beijing, 100081, China

[▽] Institut de Chimie de la Matière Condensée de Bordeaux, Avenue du Docteur Albert Schweitzer F-33608 Pessac Cedex, France

* Address correspondence to: ylu2@unl.edu, lidawei1008@gmail.com

Contents:

S1. Preparation of Sandwich-Structured Reactors for 2D MoS_2 Growth

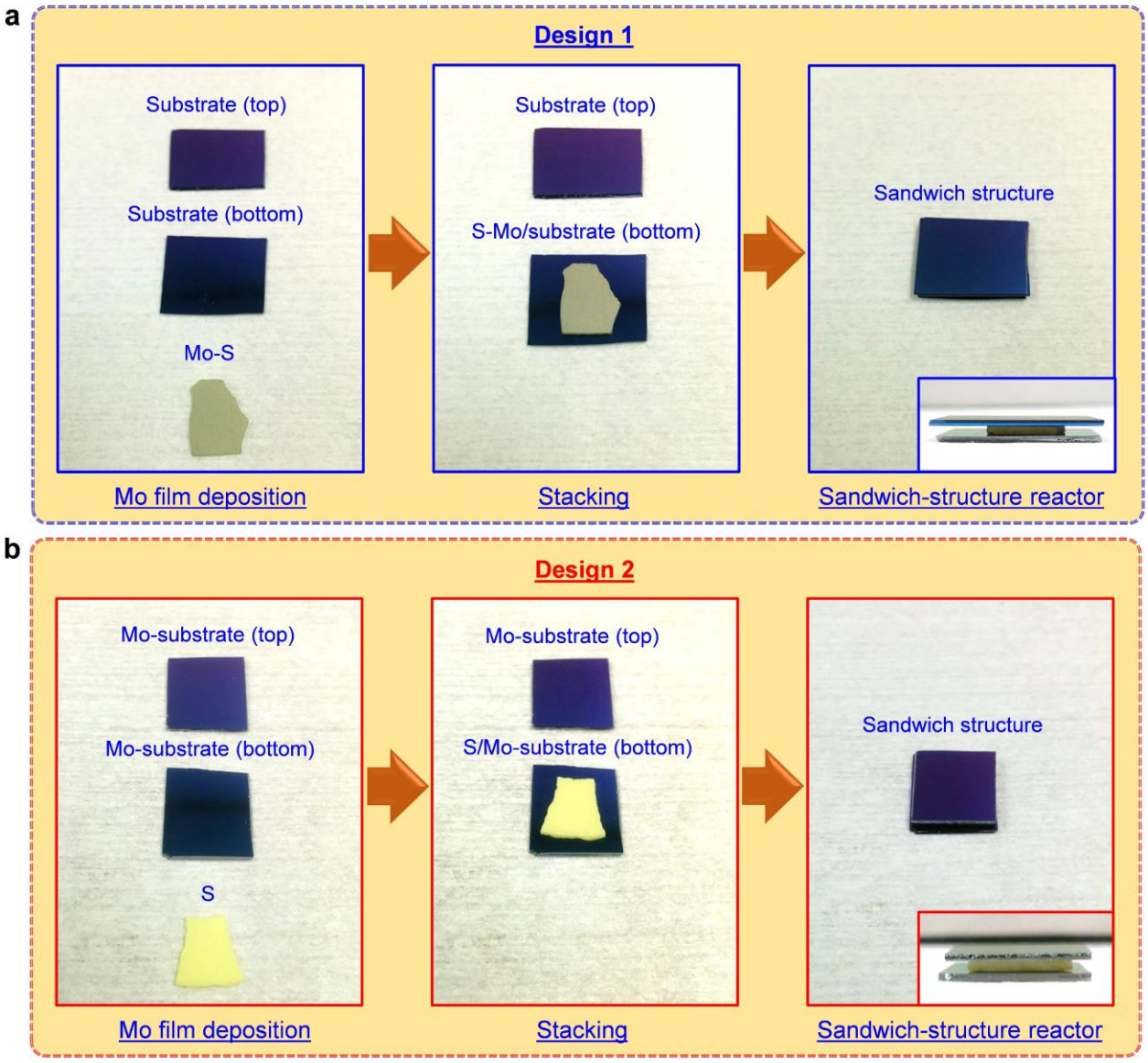

Figure S1. Preparation of sandwich-structured reactors for 2D MoS_2 growth. (a) Reactor Type 1: substrate/Mo-S/substrate sandwiched structure. (b) Reactor Type 2: substrate-Mo/S/Mo-substrate sandwiched structure.

S2. Optical Characterization of As-Grown MoS_2 Triangular Flake via Reactor Type 1

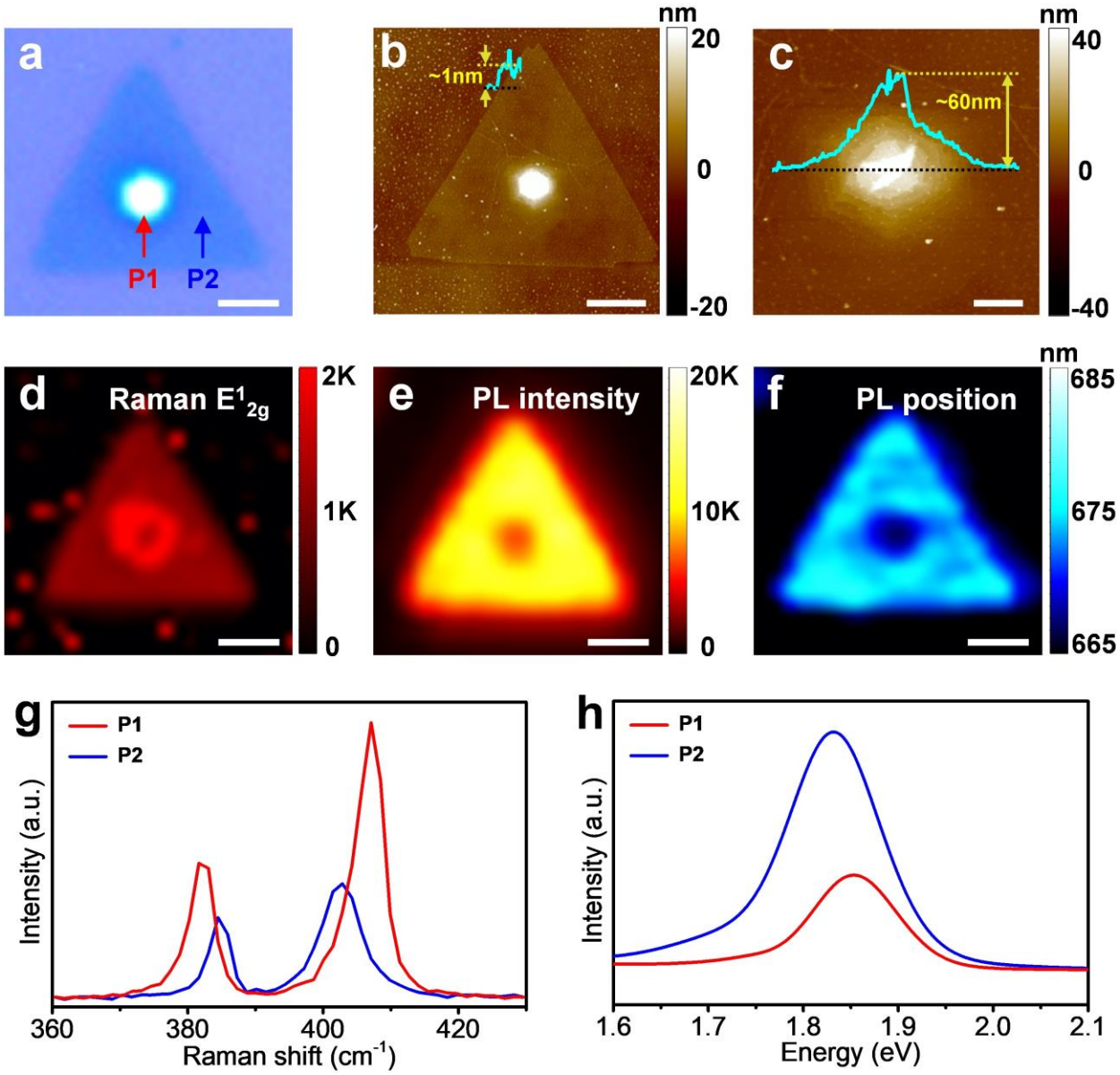

Figure S2. Optical characterization of an idividual MoS_2 triangular flake grown via Reactor Type 1. (a) Optical image; (b,c) AFM images [insets in (b,c) show the height profiles of (b) MoS_2 and (c) nucleation center, respectively]; (d) Raman intensity mapping of the in-plane E^1_{2g} band; (e) PL peak intensity mapping; (f) PL peak position mapping; (g) Raman and (h) PL spectra of the MoS_2 in the region as marked in (a). Scale bars: 2 μm for (a,b,d-f) and 500 nm for (c).

S3. Typical Examples of MoS_2 Samples Grown via Reactor Type 1

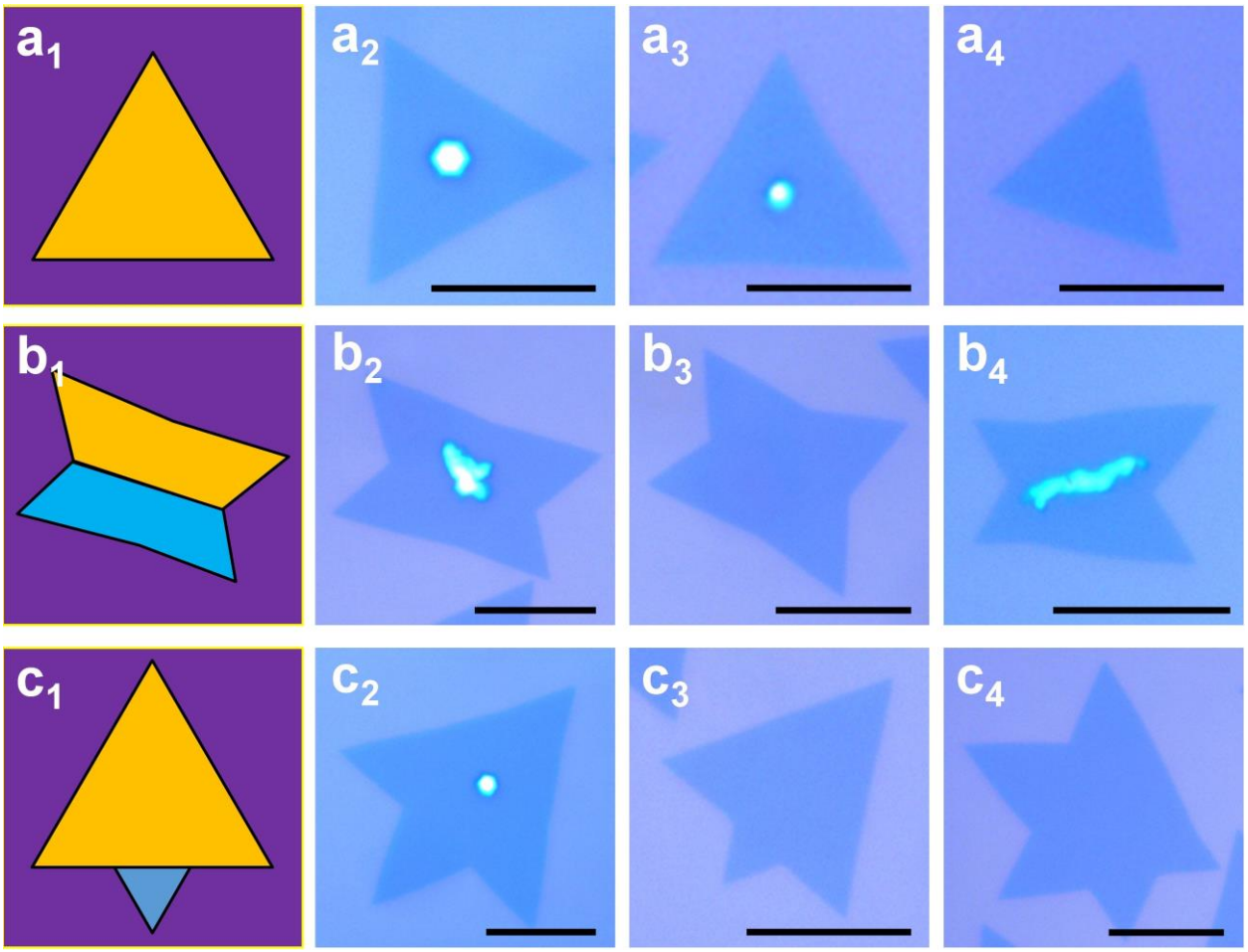

Figure S3. Typical examples of monolayer MoS_2 samples grown via Reactor Type 1. Optical images of (a_1-a_4) triangle-shaped MoS_2 monolayer, (b_1-b_4, c_1-c_4) monolayer MoS_2 with polygonal geometry (more than four angles). Scale bars: 5 μm.

S4. Optical Characterization of As-grown Monolayer MoS_2 Flake via Reactor Type 2

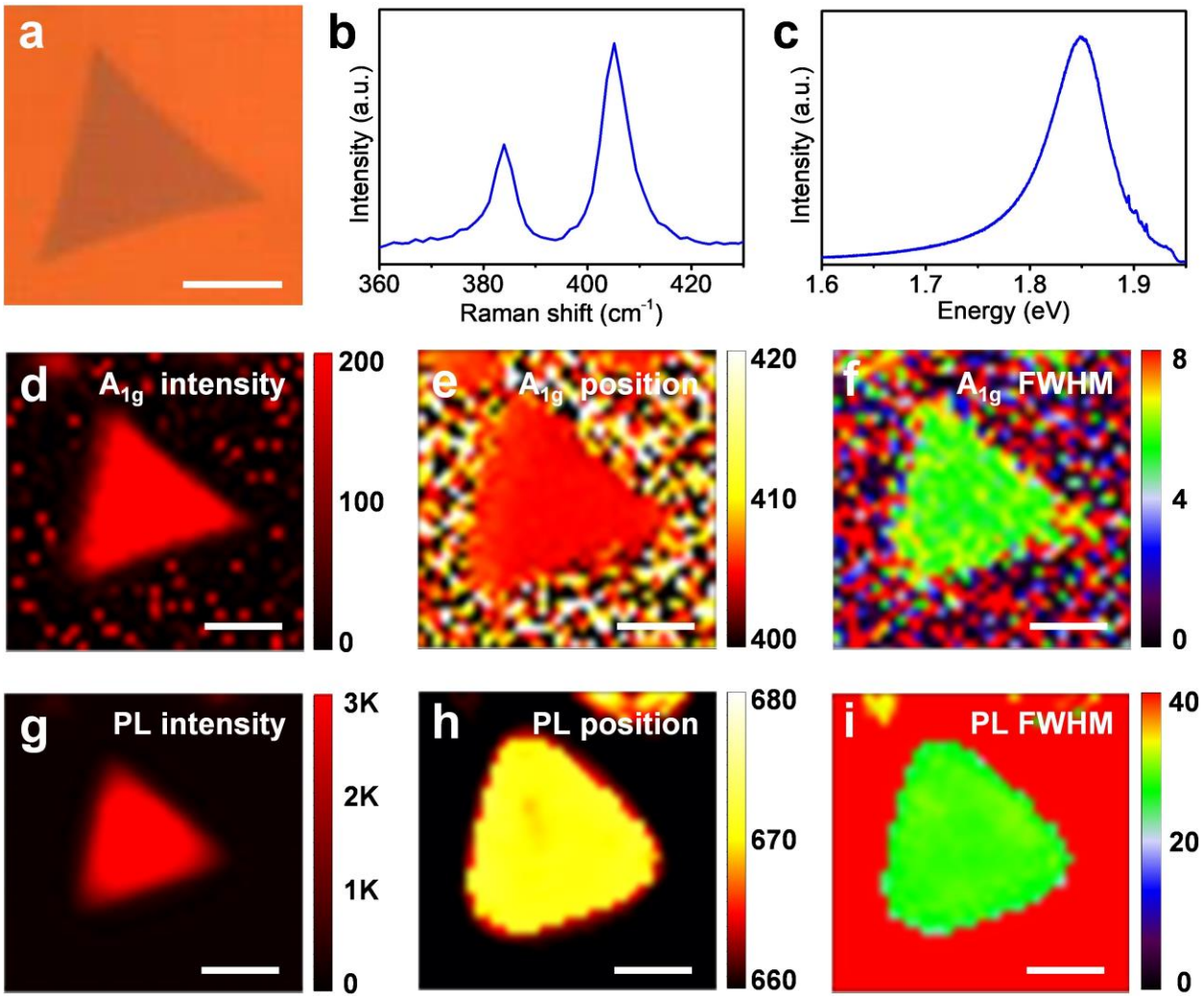

Figure S4. Optical characterization of a representative monolayer MoS_2 triangular flake grown via Reactor Type 2. (a) Optical image; (b) Raman and (c) PL spectra of the monolayer MoS_2 in (a); (d-f) Raman mapping of the A_{1g} peak (d) intensity, (e) position, and (f) full-width at half-maximum (FWHM); (g-i) PL mapping of the peak (g) intensity, (h) position, and (i) FWHM. Scale bars: 5 μm.

S5. Optical Characterization of As-grown Few-layer MoS_2 Flake via Reactor Type 2

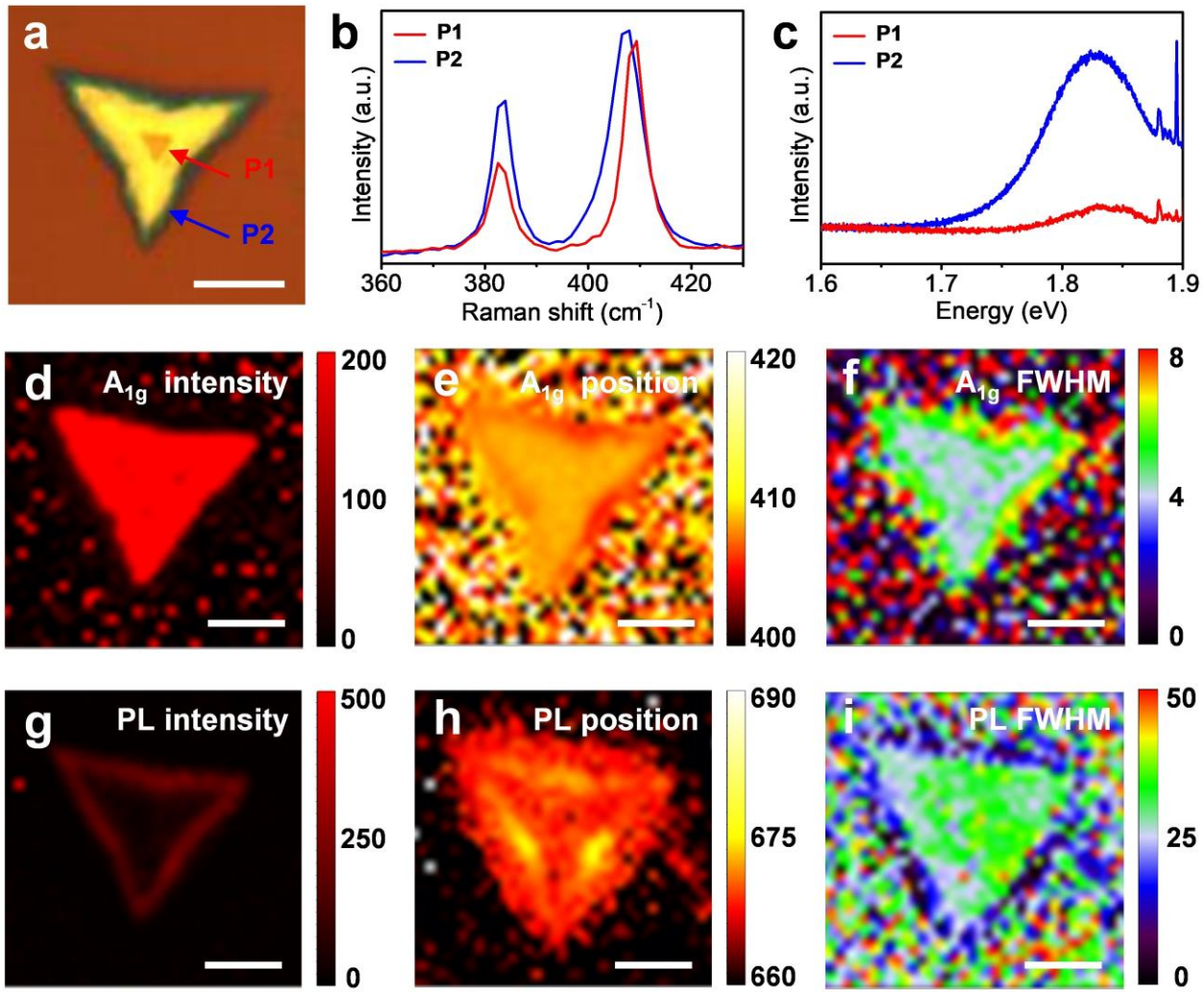

Figure S5. Optical characterization of a representative few-layer MoS_2 triangular flake grown via Reactor Type 2. (a) Optical image; (b) Raman and (c) PL spectra of the few-layer MoS_2 in the region as mraked in (a); (d-f) Raman mapping of the A_{1g} peak (d) intensity, (e) position, and (f) FWHM; (g-i) PL mapping of the peak (g) intensity, (h) position, and (i) FWHM. Scale bars: 5 μm.

S6. Typical Examples of MoS_2 Samples Grown via Reactor Type 2

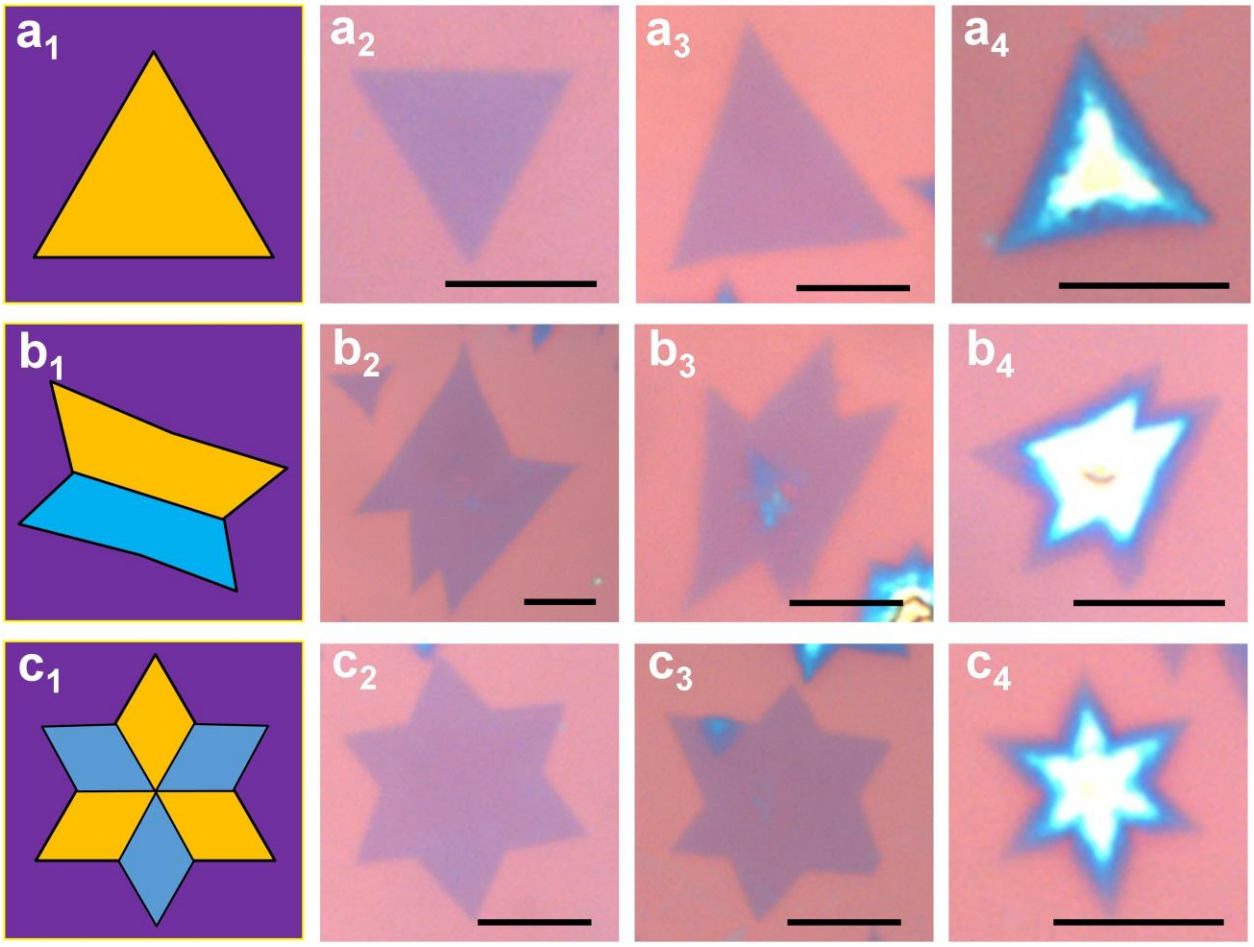

Figure S6. Typical examples of MoS_2 samples grown via Reactor Type 2. Optical images of (a_1-a_4) triangle-shaped MoS_2 monolayer and few-layers, (b_1-b_4, c_1-c_4) mono-/few-layer MoS_2 grains with polygonal geometry (more than five angles). Scale bars: 5 μm.

S7. Atomic Layered MoS_2 Grown on the Top and Bottom SiO_2/Si Substrates

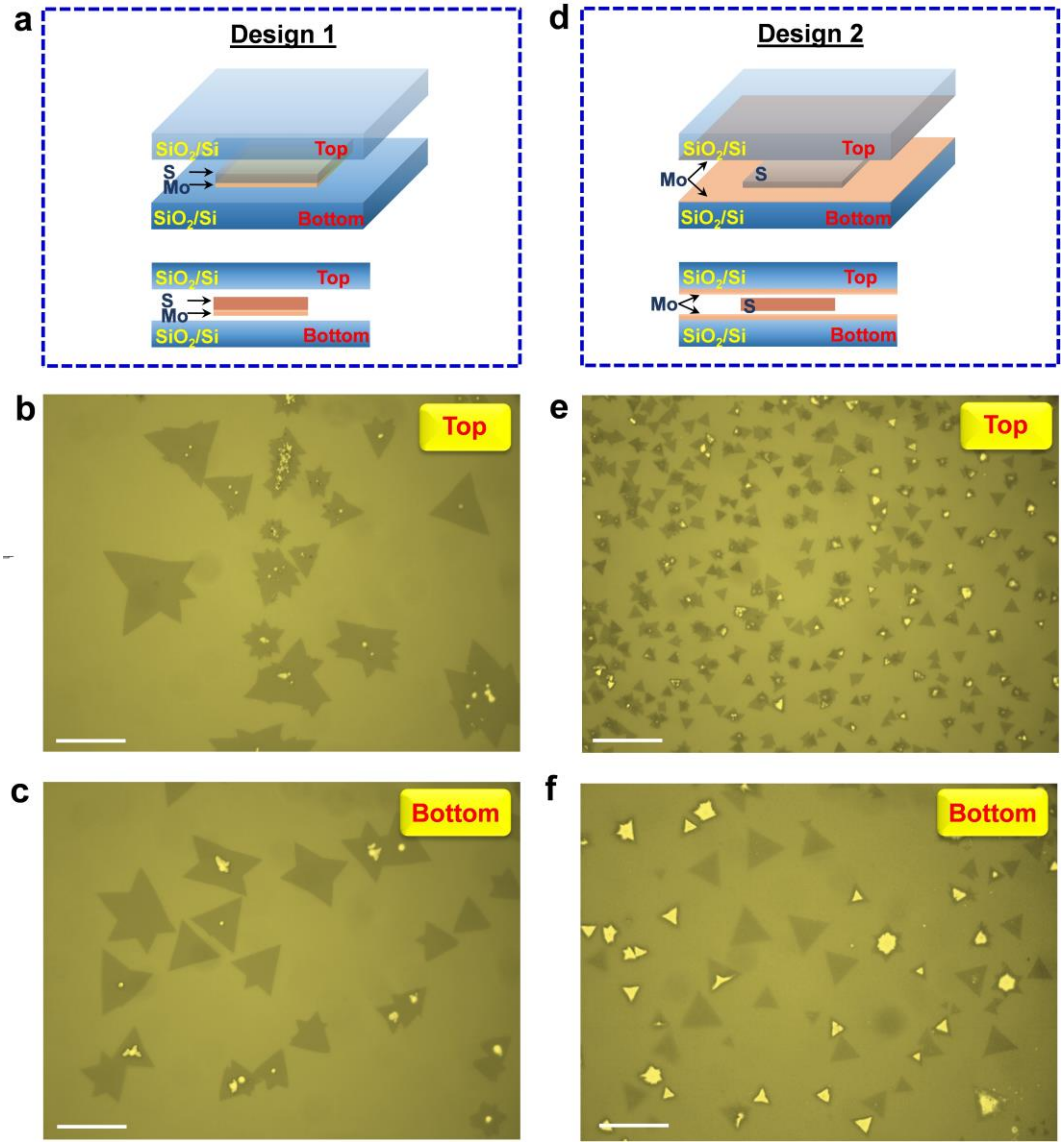

Figure S7. Schematics of two reactor configurations and optical images of the as-grown MoS_2 atomic layers. (a) Reactor 1: substrate/Mo-S/substrate. Optical images of the as-grown MoS_2 samples on the (b) top and (c) bottom sides of SiO_2/Si substrates via Reactor 1. (d) Reactor 2: substrate-Mo/S/Mo-substrate. Optical images of the as-grown MoS_2 samples on the (e) top and (f) bottom sides of SiO_2/Si substrates via Reactor 2. Scale bars: 10 μm.

S8. MoS_2 Thin Films Grown via Two Reactors Without Top Covers

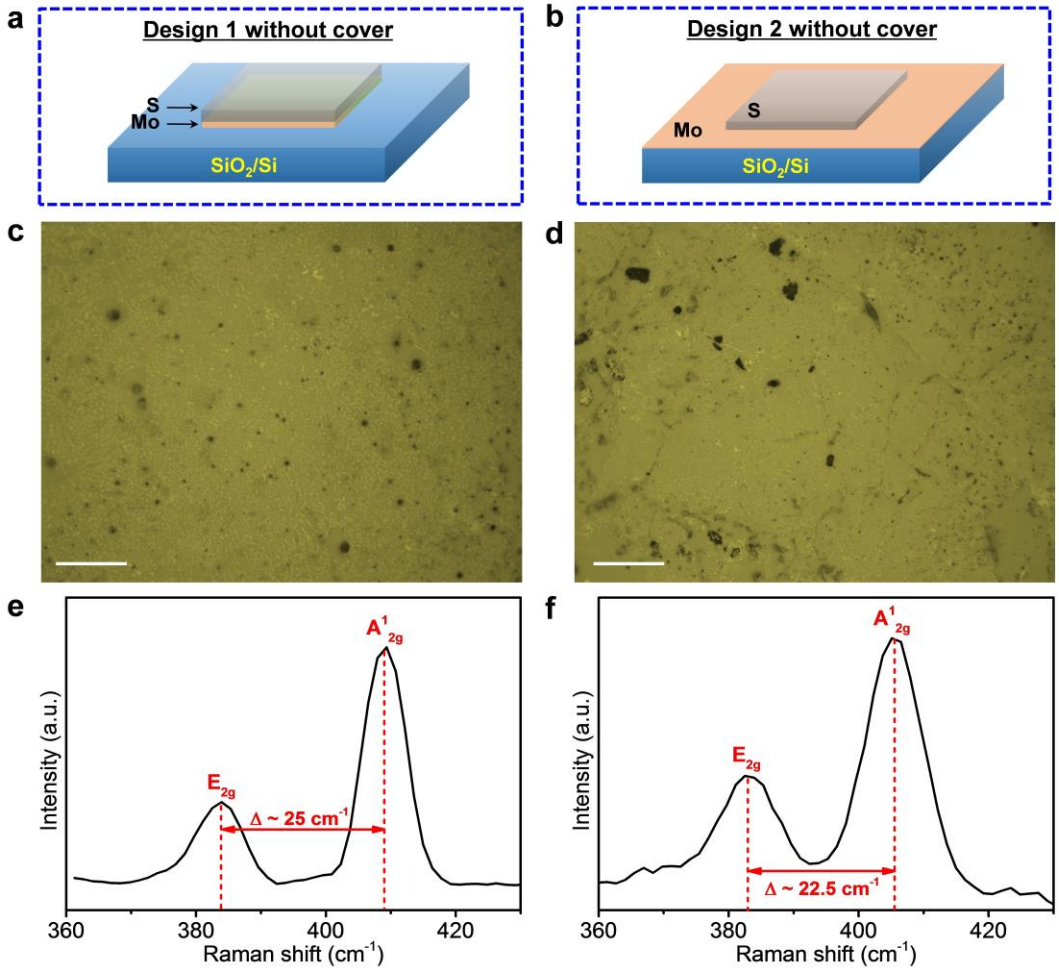

Figure S8. The as-grown MoS_2 thin films via two reactors wihout top covers. Diagrams of (a) Reactor Type 1 and (b) Reactor Type 2 without top covers. Optical images of the as-grown MoS_2 films on SiO_2/Si substrate via (c) Reactor Type 1 and (d) Reactor Type 2 without top substrates. Scale bars: 10 μm. Typical Raman spectra of the as-grown MoS_2 films on SiO_2/Si substrate via (e) Reactor Type1 and (f) Reactor Type 2 without top substrates.

S9. Phase Identification of As-Grown MoS_2 samples Via Soild-Phase Sulfurization

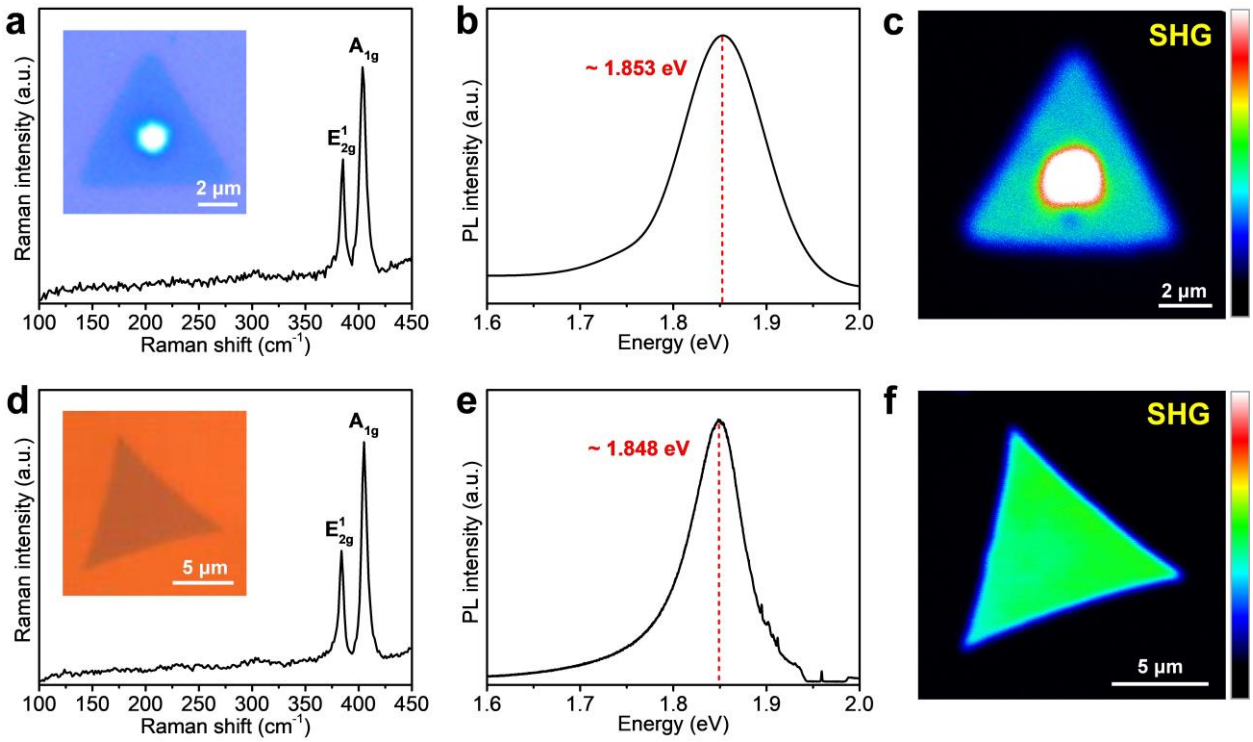

Figure S9. Phase Identification of MoS_2 samples grown via two types of sandwich reactors. (a) Representative Raman, (b) PL spectra, and (c) second-harmonic generation (SHG) intensity imaging of a monolayer MoS_2 flake shown in the inset of (a) that was grown via Reactor Type 1. (d) Representative Raman, (e) PL spectra, and (f) SHG intensity imaging of a monolayer MoS_2 flake shown in the inset of (d) that was grown via Reactor Type 2. The color bars in (c) and (f) indicate the SHG intensity.

S10. TEM Image and FFT Pattern Collected From the As-grown Single-Crystal MoS_2 Domains

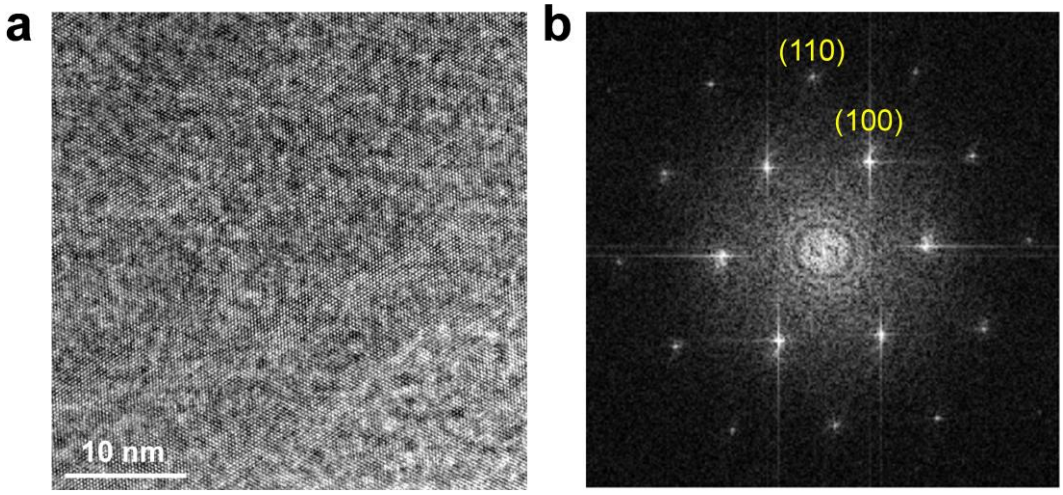

Figure S10. (a) Low-magnification TEM image of the as-grown MoS_2 single crystal. (b) Corresponding FFT image with a single set of diffraction patterns, confirming the 2H phase MoS_2 structure.

S11. TEM Charactrerzation of the MoS_2 Grain Quenched at the Initial Growth Stage

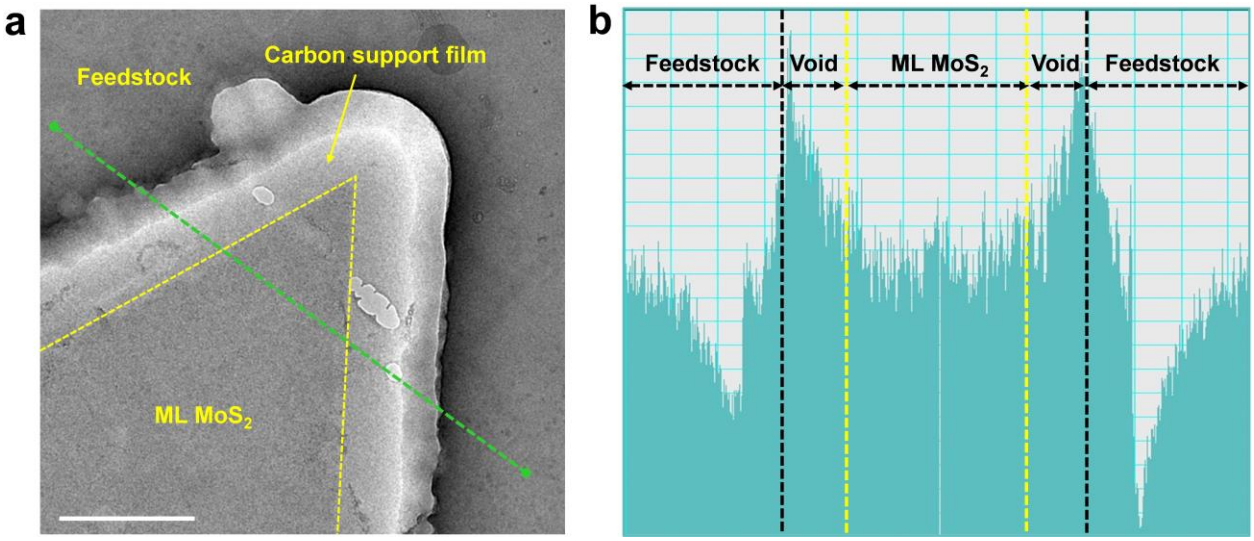

Figure S11. (a) TEM image of the crystalline edge of MoS_2 grain quenched at the initial stage of growth. The yellow dotted line indicates the edge of monolayer MoS_2. Scale bar: 400 nm. (b) Intensity profile along the green dotted line shown in (a).

S12. Theoretical Calculation of the Effect of S-Vacancies on the Work Function of MoS_2

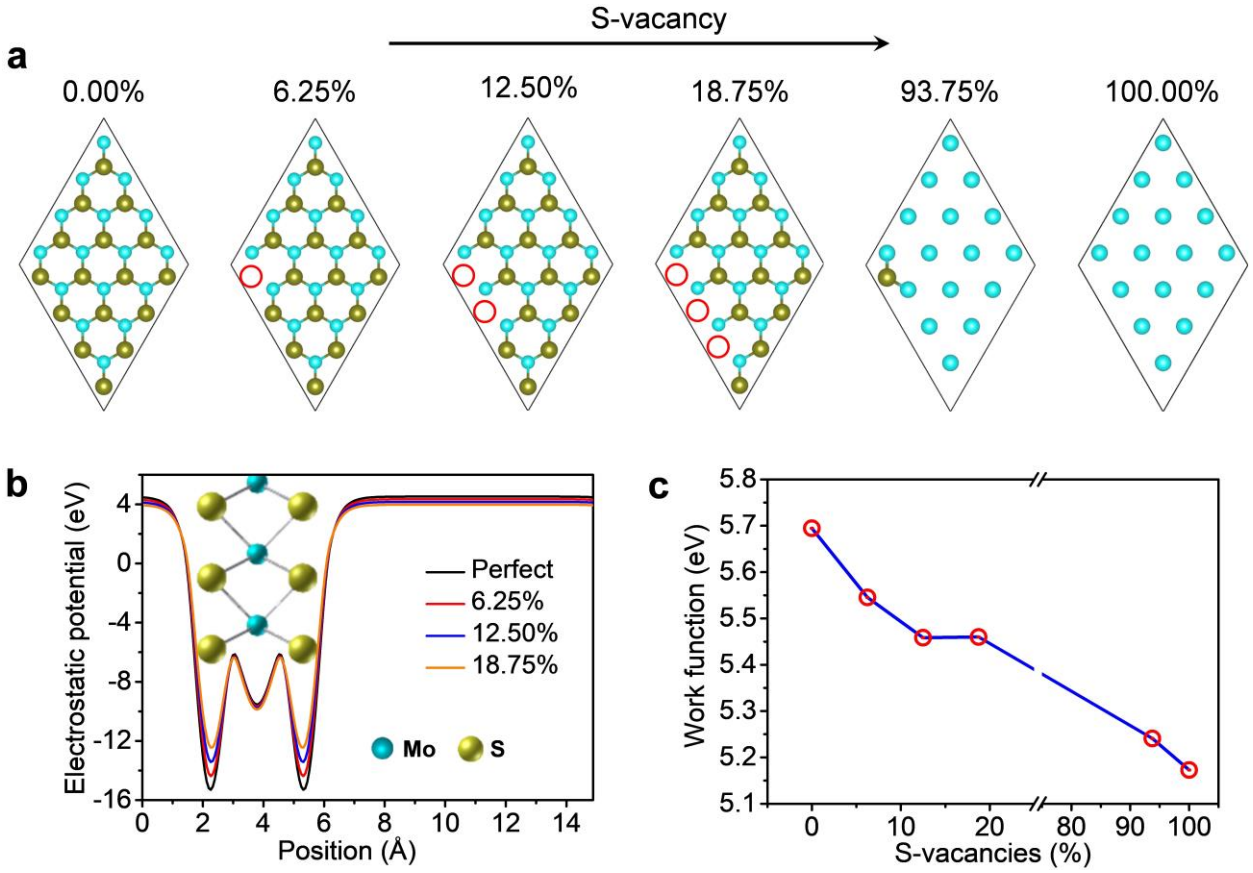

Figure S12. Theoretical caculations. (a) Structural models for monolayer MoS_2 with different concentrations of sulfur (S)-vacancies, varying from 0 to 100%. Cyan balls, yellow balls, and red opened cicles represent Mo atoms, S atoms, and S cacancy positions, respectively. (b) The electrostatic potentials of monolayer MoS_2 with different S-vacancies. (c) Work function of monolayer MoS_2 as a function of S-vacancy concentration.

S13. A Multistep Growth Model Based on the Space-Confined Solid-Phase Sulfurization

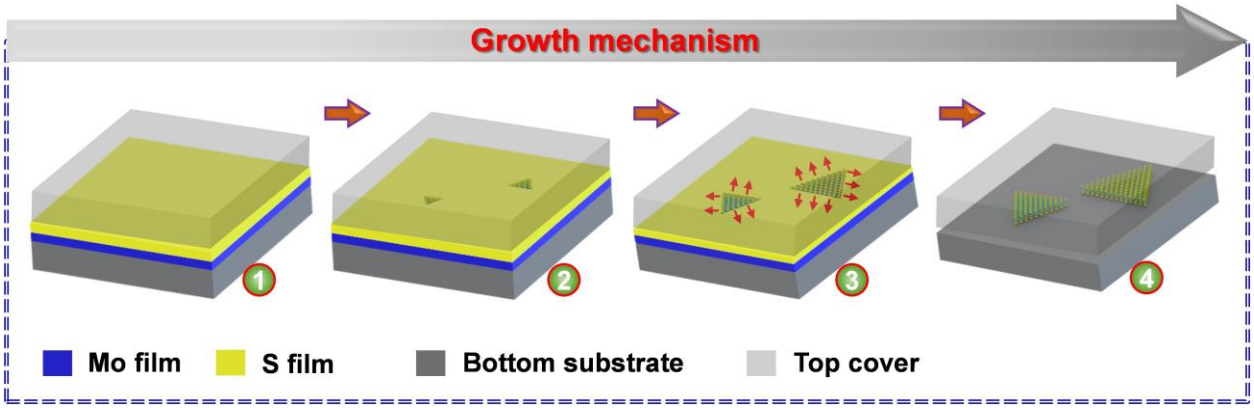

Figure S13. Schematic illustration of the proposed space-confined solid-phase growth process for monolayer MoS_2 single crystal, including 1) physical adsorption of sulfur coating, 2) nucleation, 3) lateral epitaxial growth, and 4) growth finish.

S14. AFM Characterization of the Monolayer and Few-Layer MoS_2

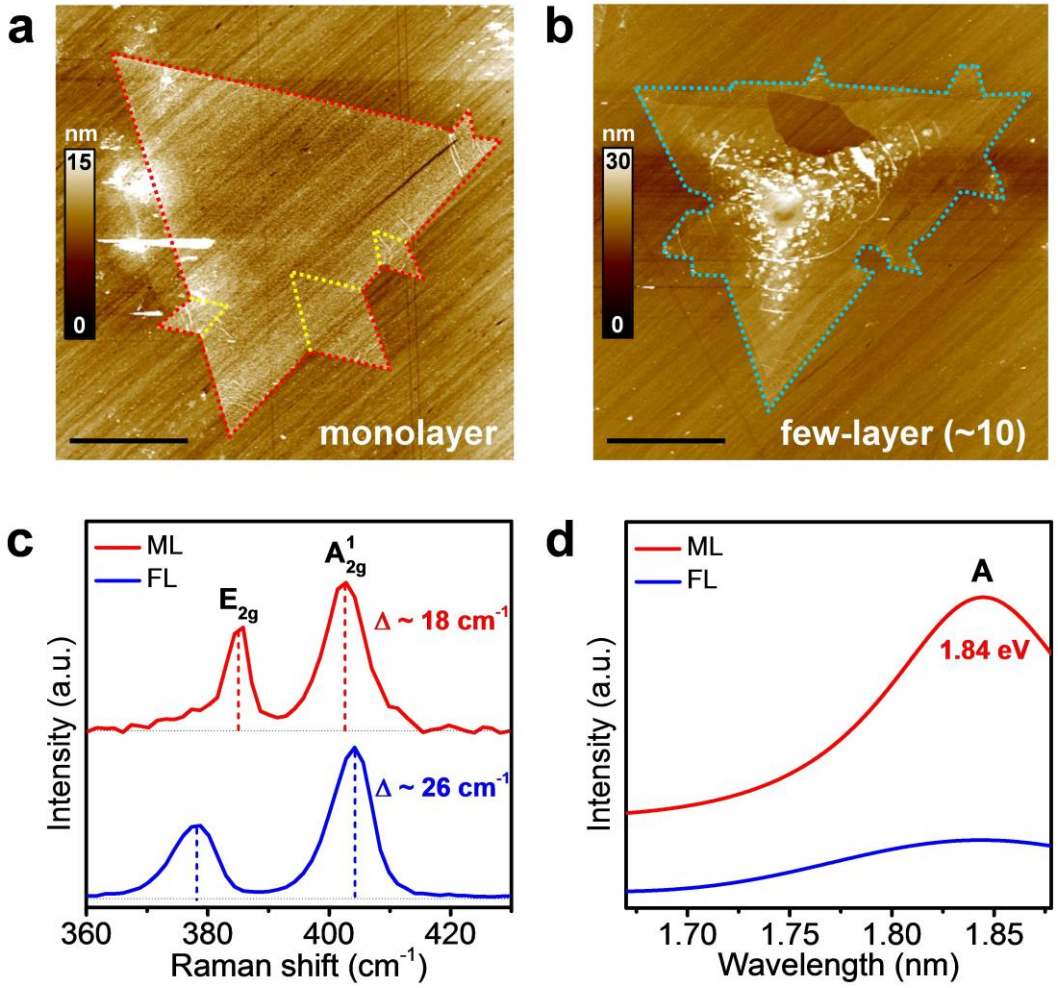

Figure S14. AFM morphologies of (a) monolayer and (b) few-layer MoS_2 as shown in Fig. 4. The dashed lines in (a,b) depict the edges of monolayer and few-layer MoS_2 flakes, respectively. Scale bars: 4 μm. (c) Raman and (d) PL spectra collected from the monolayer (red line) and few-layer (blue line) MoS_2.

S15. SHG and SFG Imaging of AA- and AB-Stacked Few-Layer MoS_2

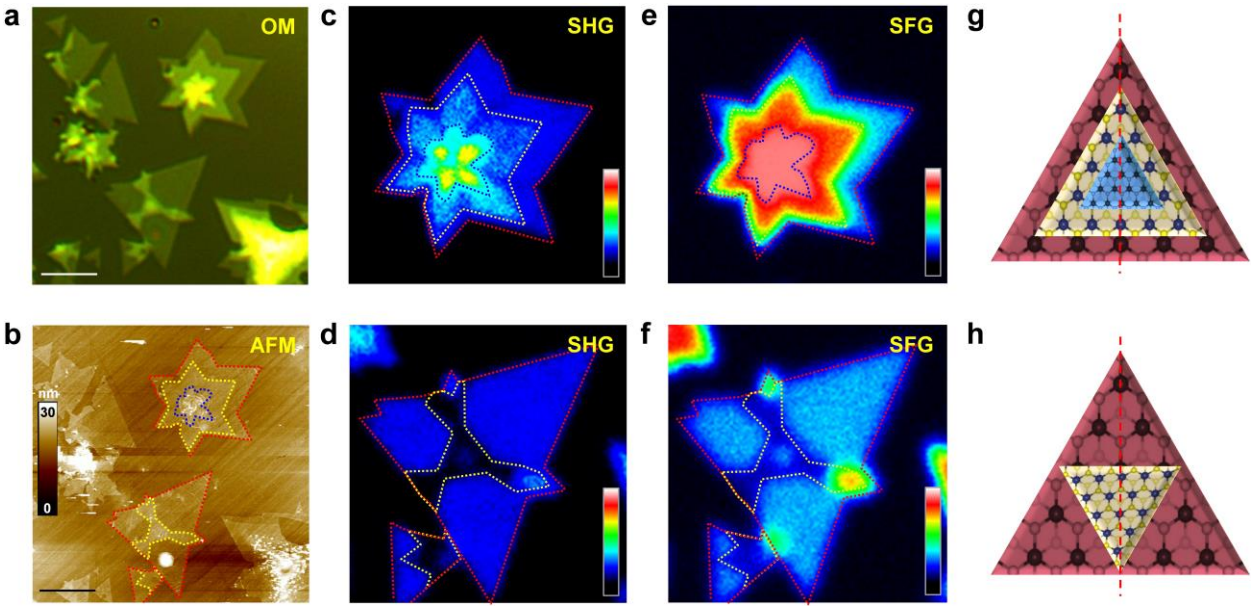

Figure S15. AA- and AB-stacked few-layer MoS_2 grown via Reactor Type 2. (a) Optical image. (b) AFM image. Scale bars: 5 μm. (c,d) SHG imaging of (c) AA- and (d) AB-stacked few-layer MoS_2. (e,f) The corresponding SFG imaging of (e) AA- and (f) AB-stacked few-layer MoS_2 shown in (c,d). (g,h) The schematic of the atomic structure of MoS_2 few-layer with (g) AA-stacking and (h) AB-stacking.

S16. Determination of Crystal Orientation of As-Grown MoS_2 Flake

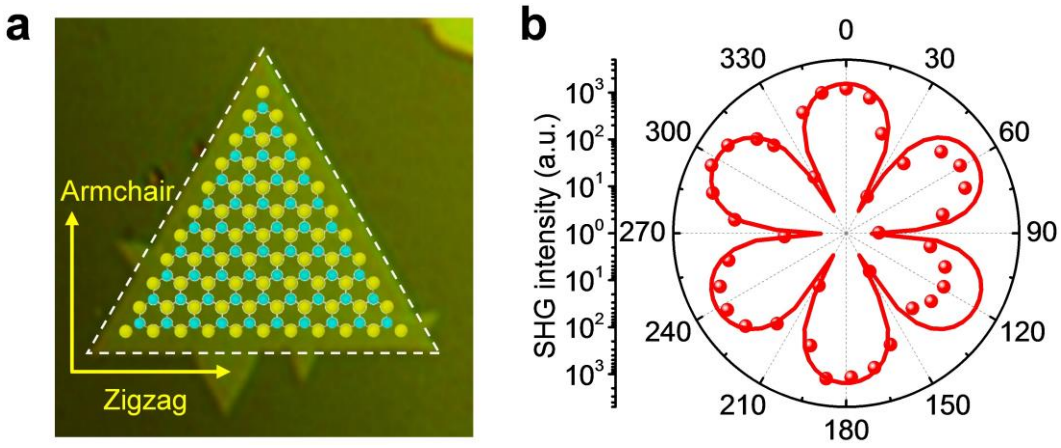

Figure S16. (a) Optical image of the as-grown monolayer MoS_2 with structural model overlaid. (b) The polar plot of the parallel polarization SHG intensity as a function of monolayer MoS_2 rotation angle.

S17. Determination of Crystal Orientation of Mechanically Exfoliated MoS_2 Crystals

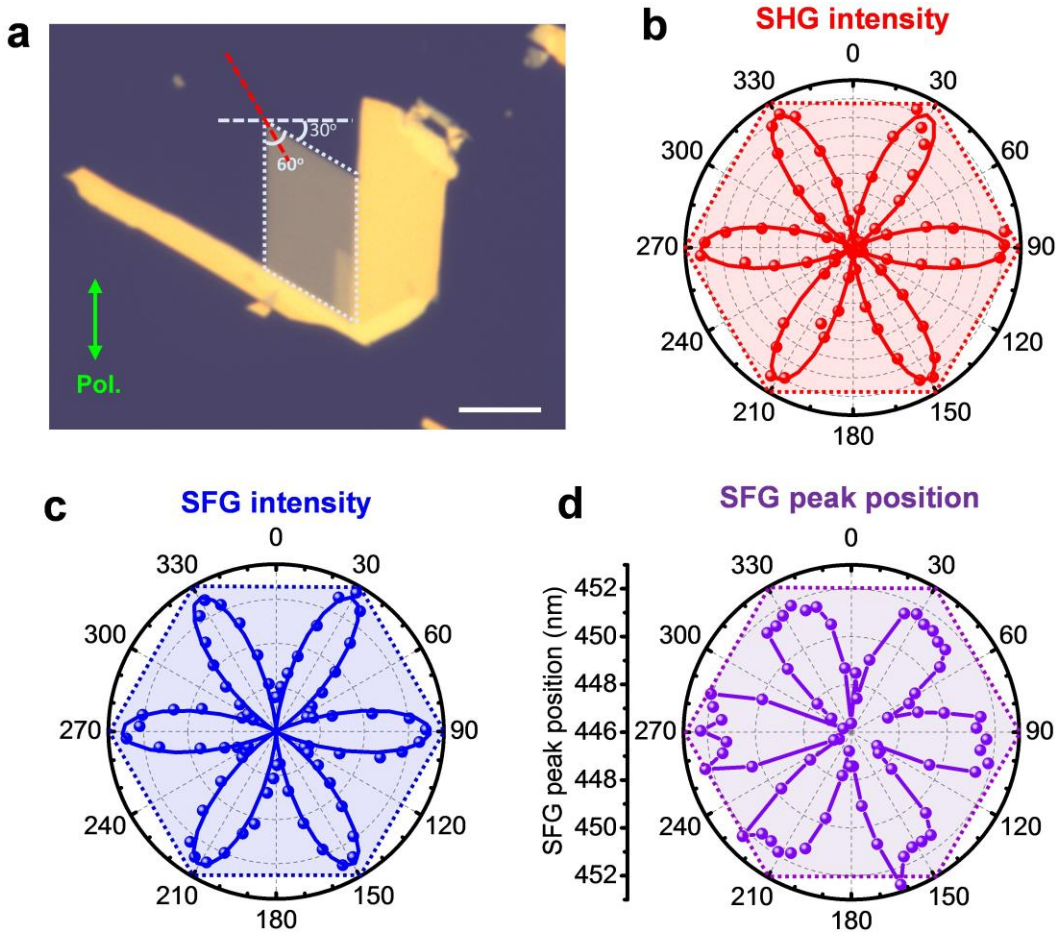

Figure S17. Measured nonlinear optical signals parallel to incident laser polarization as a function of crystal orientation. (a) Optical image of an exfoliated few-layer MoS_2 crystal. Scale bar: 5 μm. Polar plot of the (b) SHG peak intensity, (c) SFG peak intensity, and (d) SFG peak position as a function of the crystal angle.